SUPPORTING INFORMATION

Design of an Inflorescence-Type Phosphorus-doped (Ni,Co)–Molybdate Architecture with an Atomically Thin Cobalt Oxide Layer for High-Efficiency Energy Storage Systems

Sangeeta Adhikari [a,b], *Amarnath T. Sivagurunathan* [a], *Do-Heyoung Kim*[a,]*

[a]School of Chemical Engineering, Chonnam National University, 77 Yongbong-ro, Buk-gu, Gwangju 61186, Republic of Korea

[b]Catalyst Research Institute, Chonnam National University, 77, Yongbong-ro, Buk-gu, Gwangju 61186, Republic of Korea

*Corresponding author: kdhh@chonnam.ac.kr

Tel. (office): +82-62-530-1894

SUPPORTING INFORMATION

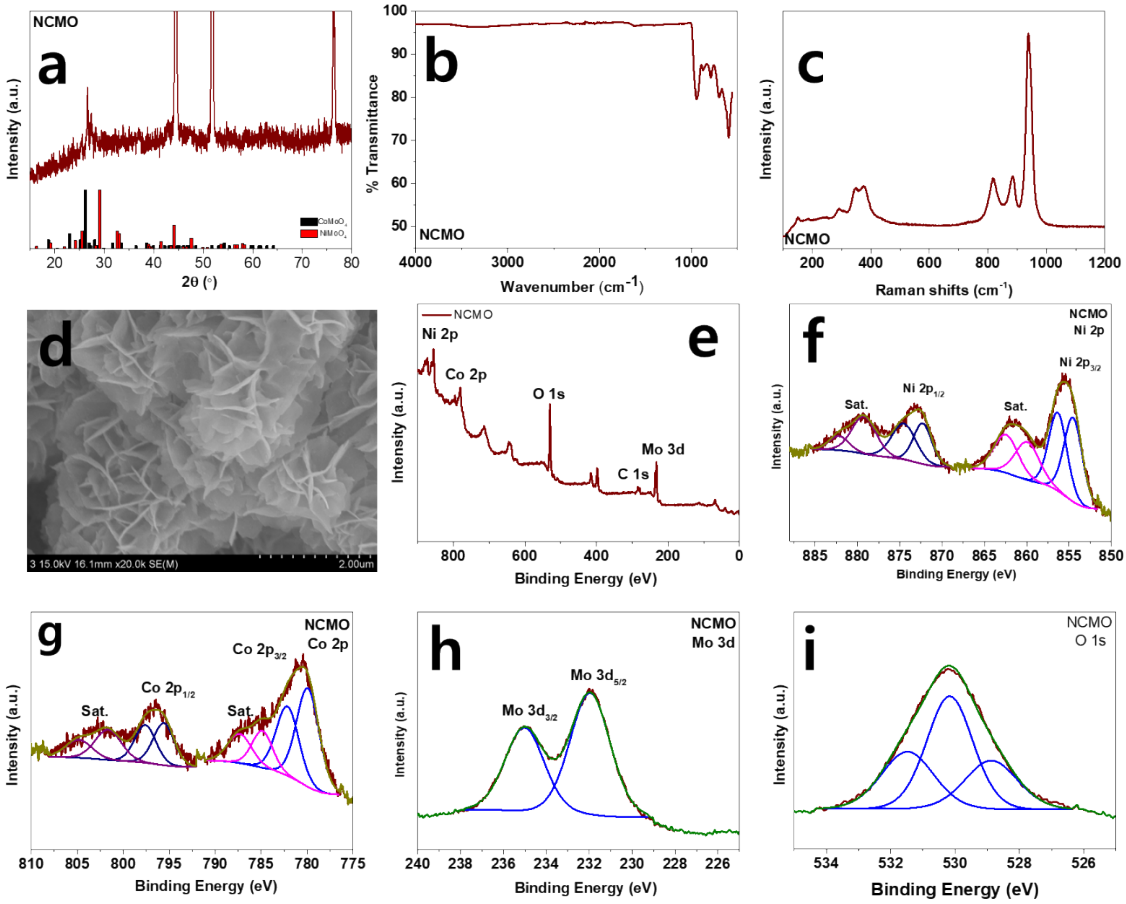

Figure S1. (a) XRD pattern, (b) FTIR spectra, (c) Raman spectra, (d) FESEM image, (e) Wide survey XPS spectrum of NCMO electrode, corresponding deconvolution of elements (f) Ni 2p, (g) Co 2p, (h) Mo 3d, and (i) O1s.

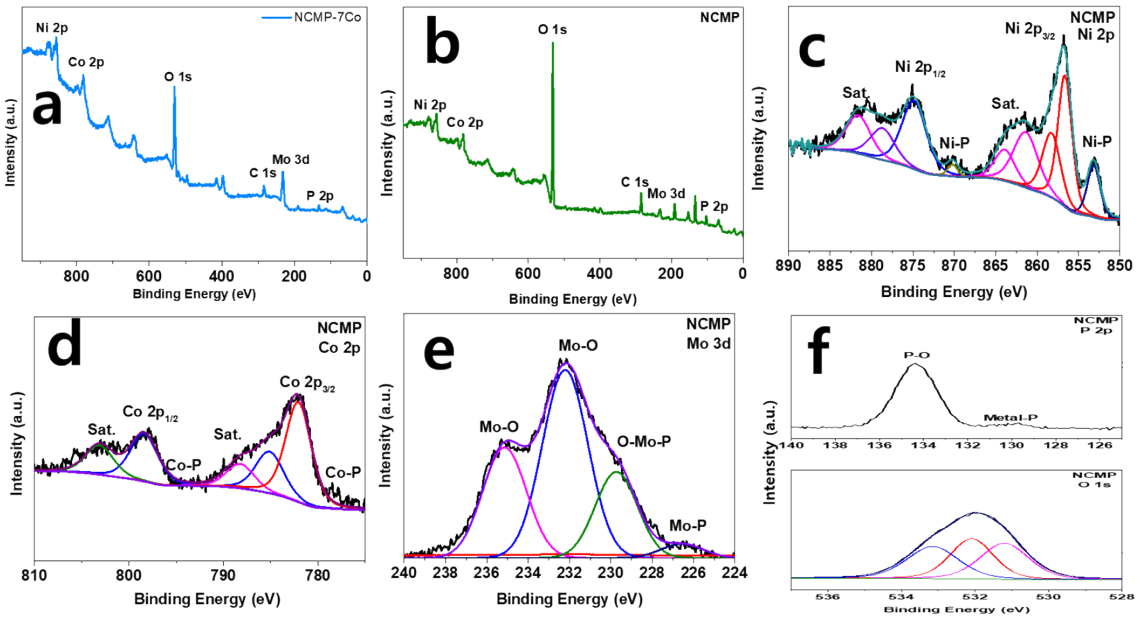

Figure S2. Wide survey XPS spectrum of (a) NCMP-7Co, (b) NCMP electrode, Deconvoluted XPS spectra of individual elements in NCMP (c) Ni 2p, (d) Co 2p, (e) Mo 3d, and (f) P 2p and O 1s.

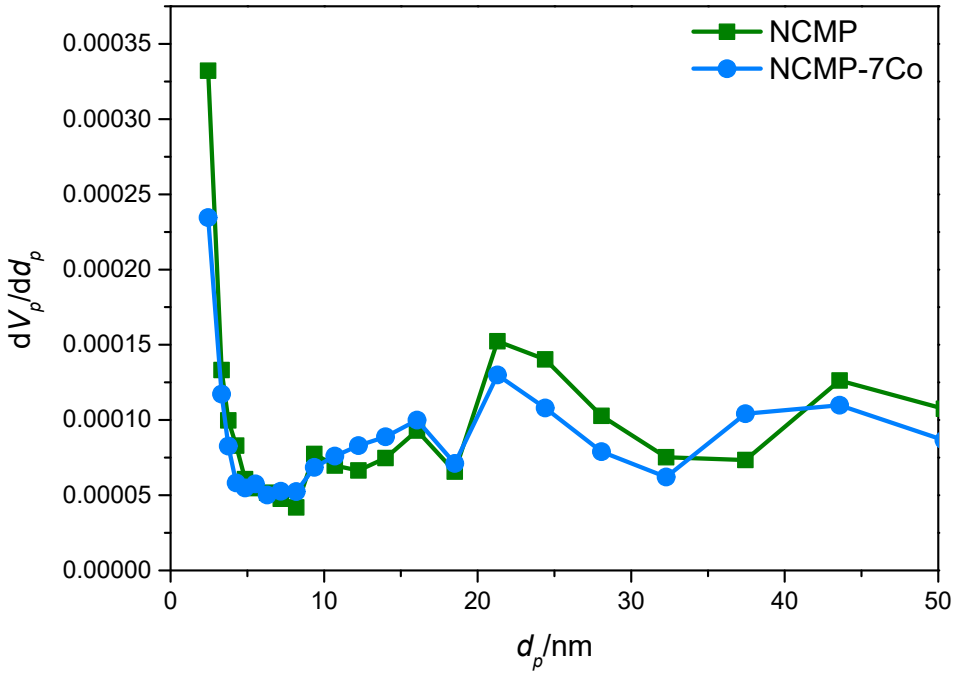

Figure S3. Pore-size distribution of NCMP and NCMP-7Co electrodes.

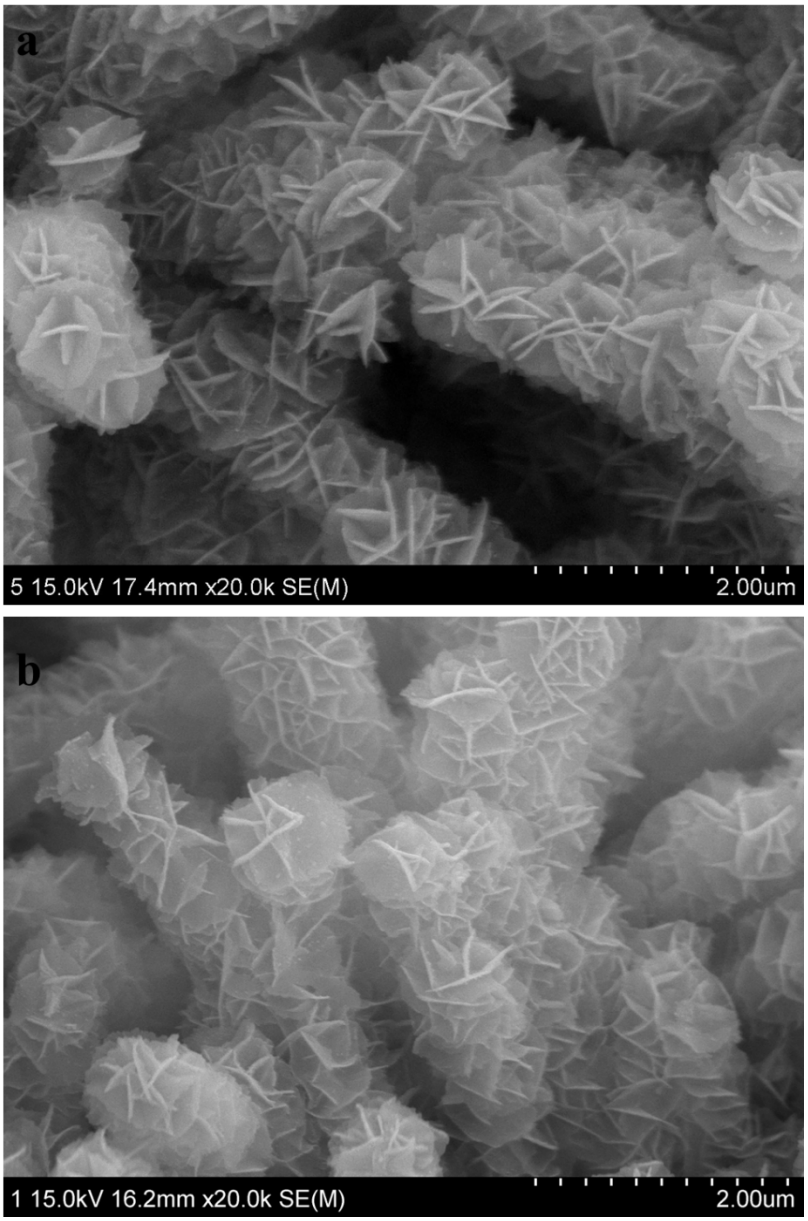

Figure S4. FESEM images of (a) NiCoMo-LDH and (b) NCMP electrode.

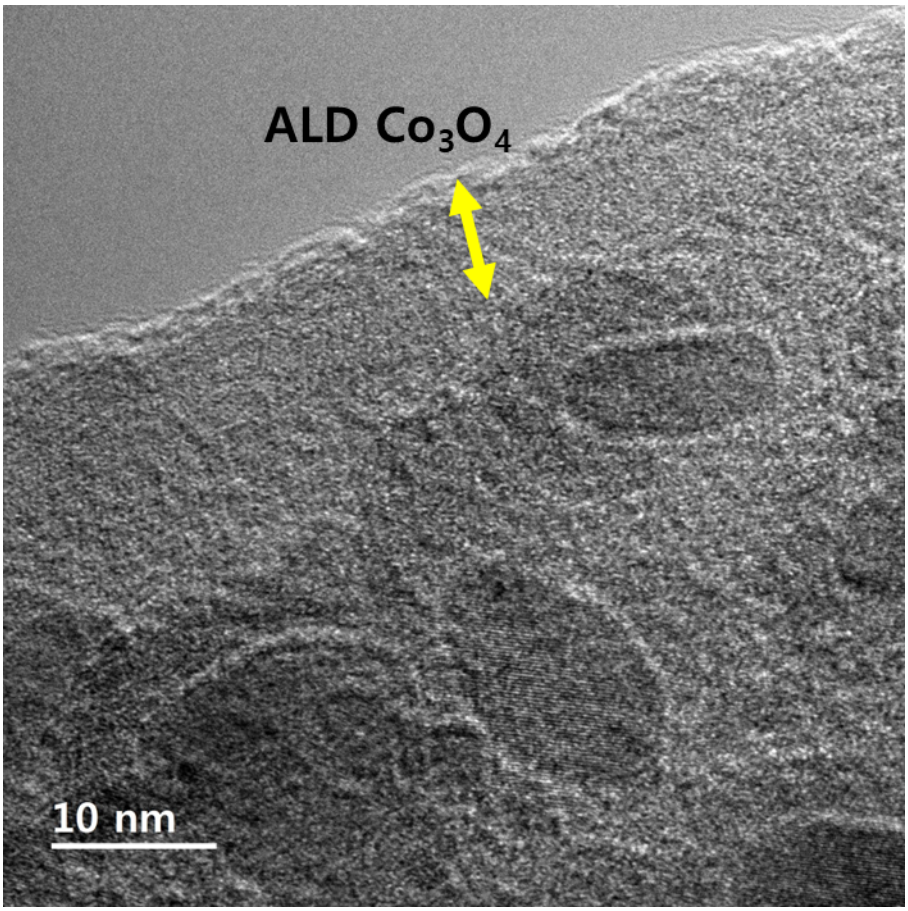

Figure S5. HRTEM image showing ALD Co_3O_4 layer with 10 nm Co3O4 coated NCMP electrode.

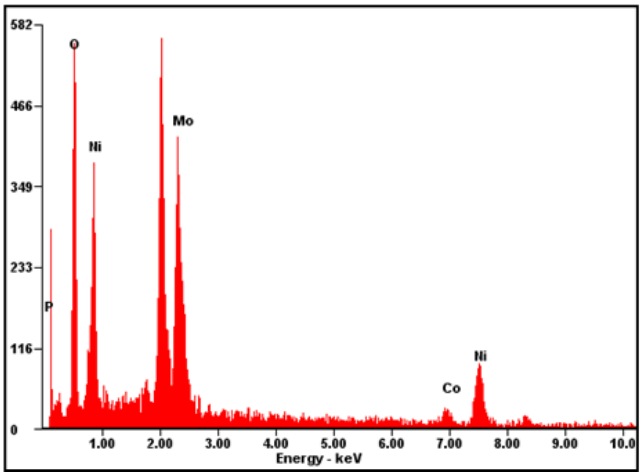

Element	*Wt%*	*At%*
OK	28.12	57.85
PK	14.99	15.93
MoL	26.04	08.94
CoK	05.78	03.23
NiK	25.07	14.05
Matrix	Correction	ZAF

Figure S6. Energy dispersive X-ray diffraction spectrum of NCMP-7Co electrode with elemental composition.

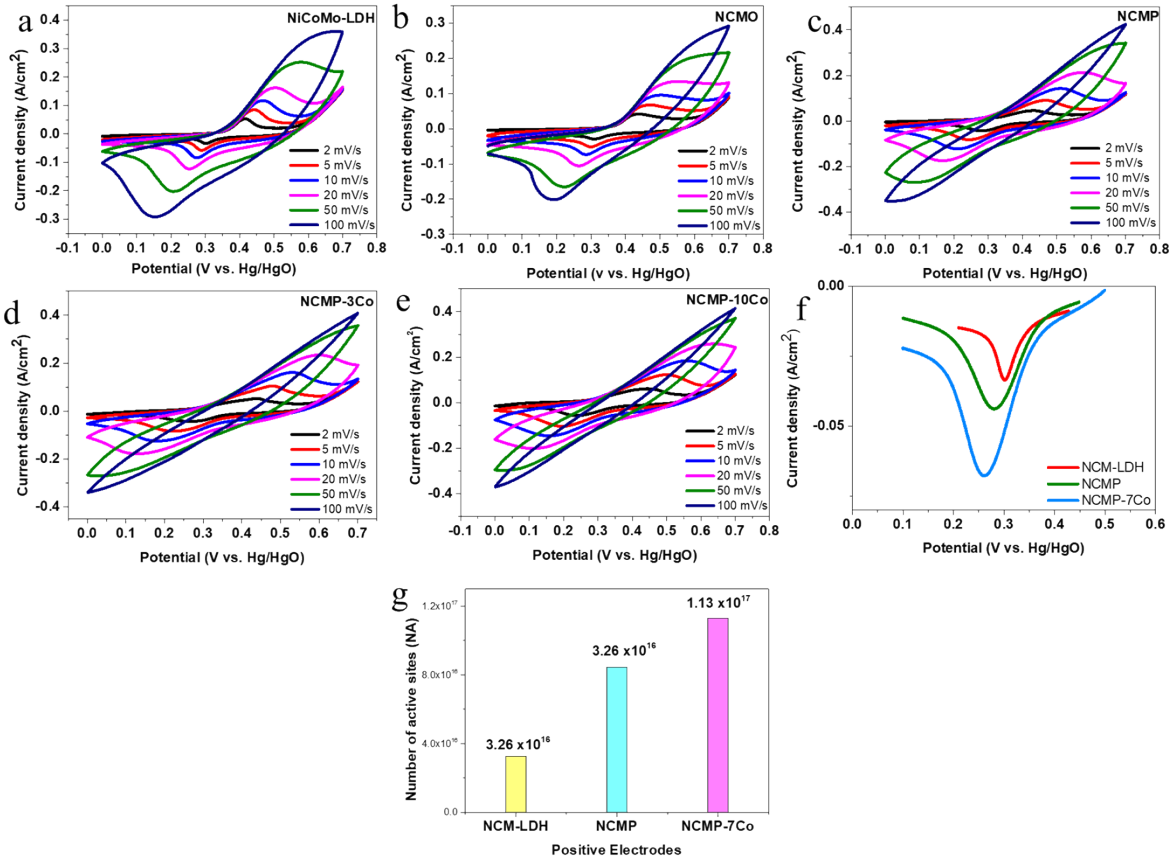

Figure S7. CV of (a) NiCoMo-LDH, (b) NCMO, (c) NCMP, (d) NCMP-3Co and (e) NCMP-10Co electrodes. (f) Reduction peak curve and (g) calculated number of active sites for NCM-LDH, NCMP and NCMP-7Co electrodes.

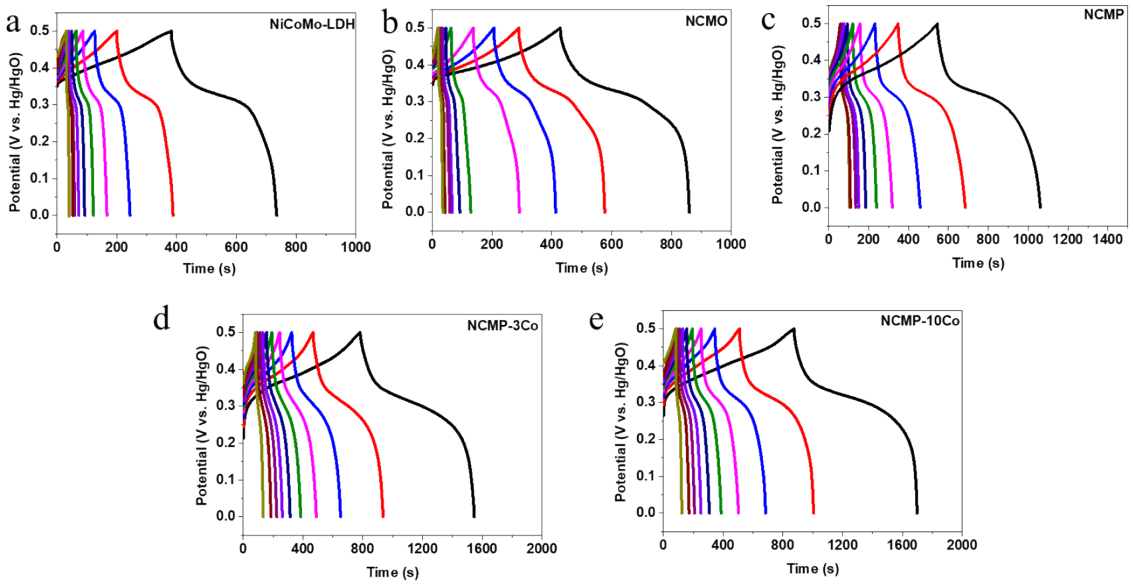

Figure S8. GCD of (a) NiCoMo-LDH, (b) NCMO, (c) NCMP, (d) NCMP-3Co and (e) NCMP-10Co electrodes.

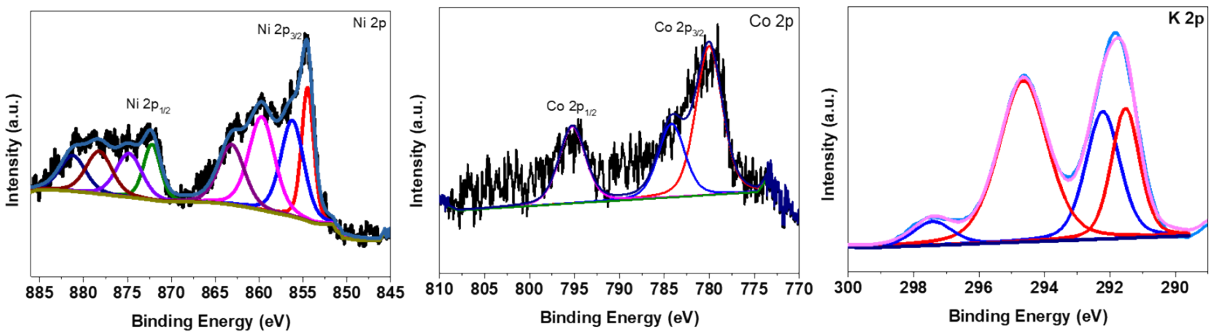

Figure S9. XPS spectra of individual elements Ni 2p, Co 2p and K 2p after 5000 charge-discharge cycles at 10 A/g current density.

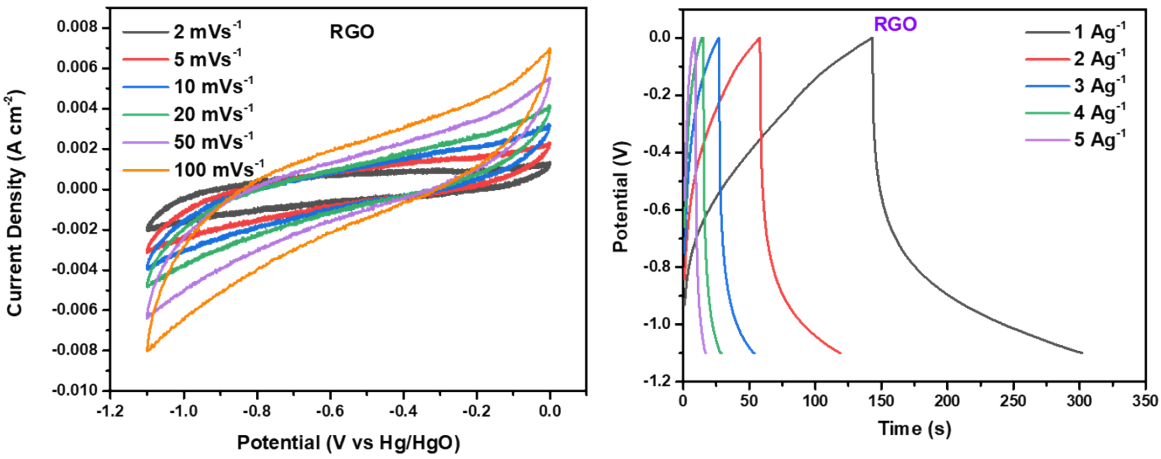

Figure S10. CV and GCD of RGO coated on Ni-foam as negative electrode.

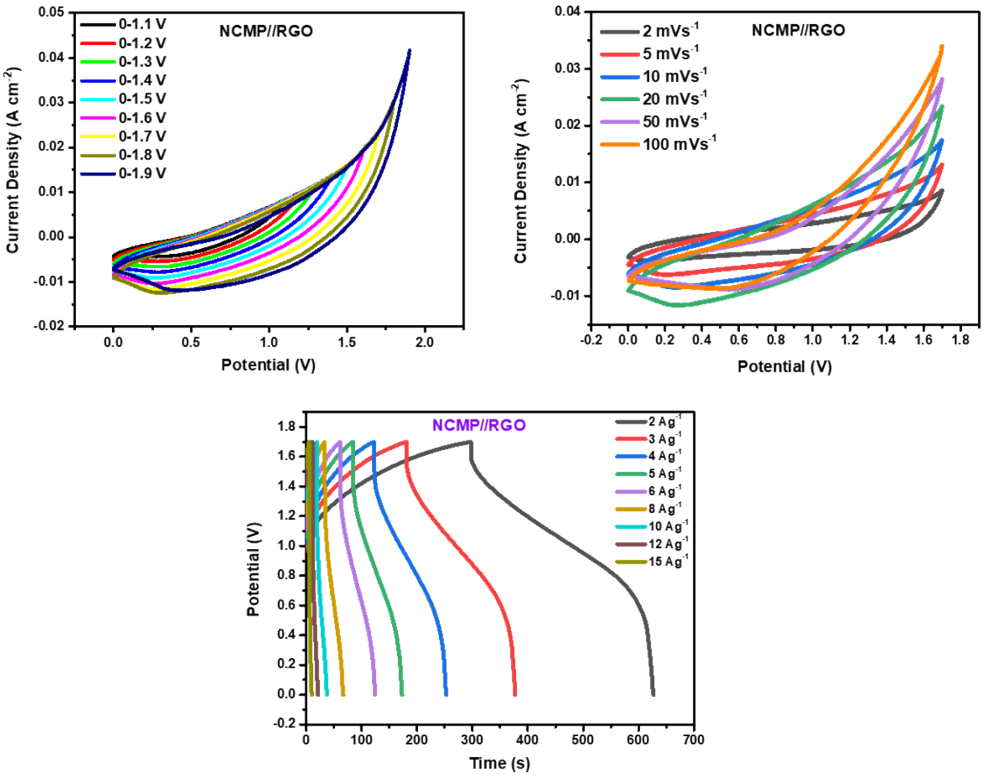

Figure S11. CV curves for the NCMP//RGO device at different voltages and a scan rate of 20 mV/s, CV curves at different scan rates over a potential range of 0 to 1.7 V, and GCD profiles at different current densities (2 to 20 A/g).

SUPPORTING INFORMATION

Table S1. Electrochemical properties and device characteristics of the with and without P-doped NiCoMo-based materials along with recent high performing materials.

	Three-electrode configuration		**Device Characteristics**					
Material	**Specific Capacity/ Capacitance**	**Electrode Stability**	**Negative electrode**	**Specific Capacity/ Capacitance**	**Energy Density**	**Power Density**	**Device-Stability**	**Ref.**
P-CoMoO4-x	1368 C/g @ 2 A/g	95.3% after 5000 cycles	Activated Carbon	220 C/g @ 1 A/g	58 Wh/Kg	850 W/Kg	98.7% after 10000 cycles	[1]
HPC/P-NCMO-2	1003 C/g @ 1 A/g	-	Activated Carbon	426.1 C/g @ 1 A/g	94.7 Wh/kg	800 W/kg	89.97% after 10000 cycles	[2]
Ni,Co-phosphate on Cu,Ni Molybdate	Areal-75.3 mAh/g	81% after 2000 cycles	Activated Carbon	46.3 mAh/g	38.2 Wh/kg	2327.5 W/Kg	87.7% after 3000 cycles	[3]
Ni_2Co_1–S-140-6	1500 F g^{-1} at 1 A g^{-1}	88.2% after 5000 cycles	PPy	368 F/g @ 1 A/g	147 Wh/kg	845 W/kg	75.9% after 5000 cycles	[4]
Ni, Co-Phosphate	891 C/g @ 1.5 A/g	97% after 4000 cycles	RGO	185 F/g @ 2.7 A/g	65.7 Wh/Kg	2.2 kW/kg	89% after 4000 cycles	[5]
NiCoP-P	1059 C/g at 1 A/g	-	Hierarchical porous carbon	145 F/g @ 0.5 A/g	51.7 Wh/Kg	-	99% after 10000 cycles	[6]
NCMP-7Co	2374 C/g @	79.8%	RGO	978 C/g @	231	1700	82.16%	This

	2 A/g	after 5000 cycles		2 A/g	Wh/Kg	W/Kg	after 4000 cycles	Work
NF@Cu@NiCoP	3401.3 F/g @ 2A/g	81.27% after 2000 cycles	Activated carbon	156.1 F/g @ 1 A/g	43.1 Wh/Kg	400 W/Kg	96.11% after 5000 cycles	[7]
P-doped $NiCo_2O_4$/$NiMoO_4$	2334.0 F/g @ 1A/g	-	Activated carbon	126.9 F /g @ 1 A/g	45.1 Wh/Kg	800 W/Kg	89.97% after 8000 cycles	[8]
CC/CoNiMn-P-500	1022 C/g @ 1 A/g	80.42 % after 2000 cycles	Activated carbon	185.85 C/g @ 3 mA/cm^2	45.7 Wh/Kg	344.8 W/Kg	84.32 % after 10000 cycles	[9]
NiCoMoS@NF	920 C/g @ 1 A/g	85.28 % after 2000 cycles	Activated carbon	107.2 C/g @ 1 A/g	35.2 Wh/Kg	800 W/Kg	83.8 % after 10000 cycles	[10]
NiCoMoS@NiCoAl hydrotalcite	1336 C/g @ 1 A/g	92.5% after 2000 cycles	Activated carbon	188.7 C/g @ 1.0 A/g	41.9 Wh/Kg	800 W/Kg	89.3% after 10 000 cycles	[11]

SUPPORTING INFORMATION

References:

[1] S. Liu, Y. Yin, D. Ni, K.S. Hui, K.N. Hui, S. Lee, C.-Y. Ouyang, S.C. Jun, Phosphorous-containing oxygen-deficient cobalt molybdate as an advanced electrode material for supercapacitors, Energy Storage Materials, 19 (2019) 186-196.

[2] Z. Cong, M. Liu, W. Li, G. Ma, K. Wang, Y. Tong, Phosphorous-doped nickel-cobalt bimetallic molybdate/three-dimensional hierarchical porous carbon for high-efficiency solid-state supercapacitors, Electrochimica Acta, 503 (2024) 144887.

[3] B. Ramulu, S.C. Sekhar, S.J. Arbaz, M. Nagaraju, J.S. Yu, Nickel–cobalt phosphate nanoparticle-layer shielded in-situ grown copper–nickel molybdate nanosheets for electrochemical energy storage, Energy Storage Materials, 44 (2022) 379-389.

[4] X. Dou, M. Liu, T. Cao, C. Wang, Y. Zhang, Y. Jia, Q. Ju, Z. Fang, Exploring the optimal post-treatment strategy for boosting the electrochemical performances of a new bimetal–organic framework-based supercapacitor, Inorganic Chemistry Frontiers, 11 (2024) 8797-8812.

[5] S.J. Marje, S.S. Pujari, S.A. Khalate, V.V. Patil, V.G. Parale, T. Kim, H.-H. Park, J.L. Gunjakar, C.D. Lokhande, U.M. Patil, Intercalation-type pseudocapacitive clustered nanoparticles of nickel–cobalt phosphate thin films synthesized via electrodeposition as cathode for high-performance hybrid supercapacitor devices, Journal of Materials Chemistry A, 10 (2022) 11225-11237.

[6] R. Liu, L. Chen, F. Mo, H. Song, G. Yang, C. Chen, X. Wu, Y. Huang, Z. Fan, Porous Cobalt-nickel phosphides prepared from Al-doped NiCo-LDH precursors for supercapacitor and electrocatalysis applications, Chemical Engineering Journal, 455 (2023) 140545.

[7] Y. Zhang, Y. Wang, Y. Feng, W. Liu, F. Chen, Amorphous nickel–cobalt phosphate nanosheets optimized by a micron−sized copper particle array with ultrahigh specific capacitance for asymmetric supercapacitors, Journal of Alloys and Compounds, 990 (2024) 174393.

[8] Y. Liu, Z. Ma, N. Xin, Y. Ying, W. Shi, High-performance supercapacitor based on highly active P-doped one-dimension/two-dimension hierarchical NiCo2O4/NiMoO4 for efficient energy storage, Journal of Colloid and Interface Science, 601 (2021) 793-802.

[9] D. Wang, F. Zhu, Y. Dang, J. Luan, M. Li, Z. Shen, D. Han, Conformal phosphating hierarchical interface of CC/CoNiMn–P for hybrid supercapacitors with high cycling stability, Inorganic Chemistry Frontiers, (2025).

SUPPORTING INFORMATION

[10] K. Zhang, H.-Y. Zeng, K.-W. Ge, M.-X. Wang, H.-B. Li, In Situ Transformation of Metal Molybdates into Polymetallic Sulfides with Enriched Edge Sites for High-Performance Supercapacitors, Inorganic Chemistry, 62 (2023) 8219-8231.
[11] K. Zhang, H.-Y. Zeng, M.-X. Wang, H.-B. Li, W. Yan, H.-B. Wang, Z.-H. Tang, 3D hierarchical core–shell structural NiCoMoS@NiCoAl hydrotalcite for high-performance supercapacitors, Journal of Materials Chemistry A, 10 (2022) 11213-11224.